

# Variable NMR Spin–Lattice Relaxation Times in Secondary Amides: Effect of Ramachandran Angles on Librational Dynamics<sup>†</sup>

John C. Williams<sup>‡</sup> and Ann E. McDermott\*

Department of Chemistry, Columbia University, New York, New York 10027

Received: March 25, 1997<sup>⊗</sup>

Deuterium NMR spin–lattice relaxation times ( $T_{1Z}$ ) of N-deuterated microcrystalline secondary amides vary from less than 1 s to more than 500 s at room temperature. The main motion effecting relaxation is an out-of-plane libration of the amide, as indicated by temperature-dependent line shapes and anisotropic relaxation spectra. Over 25 amides were measured; they vary with respect to side chain sterics, hydrogen bond lengths, hydrogen bond geometry, and crystal packing. The temperature-dependent deuterium line shape and anisotropic relaxation rates indicate an out-of-plane angular deflection of approximately  $10^\circ$ ; the angle is probably similar for the rapidly and slowly relaxing amides, while the apparent time constant for the motion probably varies dramatically. Deuterons in methylene groups on both sides of the amide group for caprylolactam and caprolactam also indicate an out-of-plane libration with relaxation rates faster than that of the amide deuteron, probably because the angular extent of the distortion is greater for the flanking  $\alpha$ -deuteron than for the amide deuteron. Carbon relaxation measurements on lauryllactam indicate that the whole molecule librates to a comparable extent. Temperature-dependent relaxation rates for caprylolactam and caprolactam showed non-Arrhenius monotonic increases in the relaxation rates with increasing temperature, as expected for libration dynamics; furthermore the quadrupolar relaxation measurements support the assumption that the dominant spectral density contribution is above the Larmor frequency (i.e.  $T_{1Q}$  is longer than  $T_{1Z}$ ). In aggregate, the data indicate that the motion effecting amide relaxation is a low-amplitude libration involving the entire molecule. Previous work on the librations of amides suggested that these librations are pronounced on the NMR time scale when the substance is near a phase transition; we report here that there is additionally a relation between the extent of libration and the structure. Comparison of the relaxation times to structures indicates that only amides with flanking alkyl groups on both sides (larger than a methyl group) exhibit extensive libration; furthermore only those amides with both flanking dihedral angles,  $\phi$   $\{C_2C_1-NC(=O)\}$  and  $\psi$   $\{N(O=C)-C_1'C_2'\}$ , near  $-60^\circ$  ( $\sim\pm 40^\circ$ ) have fast spin–lattice relaxation. On the other hand, correlation between the deuterium relaxation times and hydrogen bond length nor geometry nor crystal packing was observed. Variation in the electronic structures of the conjugated amide groups was indirectly probed by measuring the chemical shift anisotropy of the amide carbonyl carbon, the deuterium quadrupolar coupling constant, and vibrational frequencies. These parameters did not vary dramatically, indicating that the electronic structure is not strongly variable; the modest variation did not correlate with deuterium relaxation rates. The chemical shift tensor elements were  $\delta_{11} = 91.4 \pm 5$ ,  $\delta_{22} = 185 \pm 8$ , and  $\delta_{33} = 245 \pm 3$  ppm, the quadrupolar coupling constant and its anisotropy were  $203 \pm 10$  kHz and  $0.15 \pm 0.02$ , the NH stretch frequency was  $3300 \pm 42$   $\text{cm}^{-1}$ , and the carbonyl stretch frequency was  $1644 \pm 25$   $\text{cm}^{-1}$ . We suggest a model in which the shape of the local potential associated with flanking alkyl groups leads to “overdamping” of the amide librational mode and generates slower (nanosecond) components in the vibrational frequency spectrum.

## Introduction

Our understanding of librations of chemical and biochemical systems and their consequences to chemistry and macromolecular function is far from complete. The existence of low-frequency modes in proteins has been used to explain hydrogen exchange experiments in hemoglobin<sup>1</sup> and trypsin<sup>2</sup> and oxygen diffusion in myoglobin.<sup>3</sup> Low-frequency motions have been

postulated to aid chemical reactivity in solid state systems by providing directional collisions between the reactants, a phenomenon termed phonon assistance,<sup>4</sup> which has also been discussed in enzyme catalysis.<sup>5</sup> For the amide backbone in proteins one might expect a rather direct connection between low-angle fluctuations and control of function such as binding or catalysis through electrostatic terms; the charge-separated resonance structure of the amide produces a substantial dipole moment and any motions of the amide modify the frequency dependence of the local dielectric constant of proteins in a substantial way. Systematic studies identifying or characterizing low-frequency motions and their dependence on structure are still lacking.

This study reports solid state NMR measurements of librational dynamics of secondary amides. Amides are known to

<sup>†</sup> Acknowledgment is made to the Donors of the Petroleum Research Fund, administered by the American Chemical Society, for partial support of this research. A.E.M. acknowledges support from Kanagawa Academy of Science and Technology and National Institutes of Health GM50291. J.C.W. acknowledges support from NIH Biophysics training grant GM98281.

<sup>‡</sup> Currently at the European Molecular Biology Lab, Meyerhoffstrasse 1, D69012 Heidelberg, Germany.

\* To whom correspondence should be addressed.

<sup>⊗</sup> Abstract published in *Advance ACS Abstracts*, July 1, 1997.

librate out of plane in a range of 8–15° in small molecules and in proteins. For isolated molecules, the frequency of out-of-plane librational modes would be expected to be in the far infrared region (10–200 cm<sup>-1</sup>), much too high to provide an NMR relaxation mechanism and probably too fast to impact function of biopolymers. In the condensed phase and in macromolecules in particular, librational modes with amide rocking character can be observed on dramatically slower time scales. The lower frequencies in the condensed phase can be explained in a variety of ways. Formation of hydrogen bonds to adjacent groups could restrict the extent of excursion of the amide from its equilibrium position; conformations of adjacent methylene groups and attached bulky side chains may also affect the time scale, and coupling of modes from neighboring groups (for example electrostatically) might induce collective motions and lower the frequency.

Previous studies of libration in proteins involved a wide variety of experimental approaches, mainly sensitive to fast time scales. Raman spectroscopy,<sup>6,7</sup> inelastic neutron scattering techniques,<sup>8</sup> dielectric relaxation,<sup>9</sup> and acoustical methods have provided information about crystalline dynamics, particularly for frequencies in the giga- to tetrahertz regime. Computational studies such as molecular dynamics and normal mode calculations have also provided detailed information about these modes,<sup>10,11</sup> and they too have mostly concentrated on motions in the tens of nanoseconds to femtosecond regime. Solid state NMR methods can extend these measurements to the giga- to kilohertz regime.<sup>12–14</sup> SSNMR methods can be useful for detailed studies of biopolymers when specific isotopic labeling is possible.

An unexpected variability in the librational dynamics of the amide plane among 25 secondary amides is reported herein, which seems to be related to the presence of torsional angles of the flanking alkyl groups. Compilation of the relaxation times of the amidic deuteron with many other properties possibly related to hydrogen bond strength fails to yield a correlation with motion time scale; these include the intramolecular conformation, hydrogen bond length and geometry, crystal packing geometry, and spectroscopic signatures; i.e., the quadrupolar coupling constant of the deuteron, its anisotropy,<sup>15–18</sup> <sup>13</sup>C chemical shift anisotropy, and infrared frequencies. A model for the motion is discussed in which the relation between flanking torsional angles and time scale of fluctuation is addressed.

## Experimental Section

**Sample Preparation.** Samples were either purchased from Aldrich or Janssen or synthesized. Several amides were synthesized (*N,N'*-heptamethylene dibenzamide, *N,N'*-hexamethylenediacetamide, *N,N'*-hexamethylenedibenzamide, *N,N'*-heptamethylenedipropionamide, *N,N'*-octamethylenedibenzamide, *N-tert*-butylacetamide, *N-tert*-butylpropionamide, *N,N*-di-*n*-butyladipamide, and *N,N*-isopropyladipamide) by reacting 1 equiv of the appropriate acid chloride with 1 equiv of the appropriate amine in a solution of triethylamine and methylene chloride or ether and cooling in a dry ice/acetone bath.<sup>19,20</sup> *N-tert*-butylacetamide is a typical example. An oven-dried, three-neck round bottom flask was equipped with an equal pressure dropping funnel and a stir bar with dry nitrogen gas purge. A solution of *tert*-butylamine (14.5 mL/0.138 mol) and ether (20 mL) was placed in the round bottom flask and cooled in a dry ice/acetone bath. When ether was used as a solvent, *tert*-butylamine was added in 2-fold excess to neutralize the chloride. For other syntheses, freshly distilled triethylamine was used to neutralize the chloride. The acetyl chloride (4.9/0.069

mol) was placed in the dropping funnel and added over a period of 15 min to the amine/ether solution. A white precipitate was seen after the first drop. The solvent was removed by rotary evaporation, and the solid was dissolved in methylene chloride. The methylene chloride was then washed several times with a 5% sodium bicarbonate solution. The organic layer was separated, pooled, and evaporated under reduced pressure. The resulting white crystalline material was then recrystallized several times with methanol. The NMR and IR confirmed the formation of an amide. The final yield was 5.1 g or 64% (0.044 mol). In certain cases, a light orange solution of viscous material resulted, and sublimation under reduced pressure and heat provided pure material. Solution <sup>1</sup>H NMR, <sup>13</sup>C solid state NMR, and infrared measurements indicated the desired product. Polyamide-4,6 was generously provided to us from Dr. I. Vulic', DSM.<sup>21</sup>

The amidic proton of each sample was exchanged in D<sub>2</sub>O or ethanol-*d*. The exchanged samples were recrystallized in the same solvent as reported in the crystal structure, and the IR of each amide indicated better than 75% deuteration in each case.

**Preparation of  $\alpha$ -Deuterio Compounds.** The  $\alpha$ -deuterated compounds were prepared from the parent cycloketone and hydroxylamine hydrochloride via the Beckman rearrangement. The following procedure resembles closely that used for the  $\alpha$ -deuterated caprolactam. The  $\alpha$ -deuterons of the cyclooctanone were exchanged twice in NaOD/CH<sub>3</sub>OD/D<sub>2</sub>O. The exchange was monitored via solution <sup>1</sup>H NMR { $\alpha$ CH first exchange (CDCl<sub>3</sub>, 88% D)  $\delta$  ppm = 2.32 triplet of triplets; second exchange, undetected}. Hydroxylamine hydrochloride was exchanged twice in D<sub>2</sub>O and dried by rotary evaporation. The exchanged hydroxylamine (1.89 g) was added to 5 mL of D<sub>2</sub>O and slowly neutralized with anhydrous potassium acetate (2.68 g). To this solution was added the exchanged cyclooctanone in 8 mL of methanol-*d*. The solution was refluxed with gentle stirring for 3 h. The solution was then cooled and extracted three times with chloroform. The chloroform extract was dried by rotary evaporation, producing a white crystalline material. Proton NMR of a protonated control at this point indicated the formation of the oxime due to the splitting of one of the  $\alpha$ -carbon's protons { $\alpha$ CH = triplet;  $\delta$  = 2.36, 2.40, 2.43 and 2.19, 2.22, 2.25}. A solution of hydrosulfuric acid and water (10:2 v/v) (3 mL) was added to the crystalline material and gently heated until a deep orange solution resulted. The solution was neutralized with sodium hydroxide and extracted three times with chloroform. The chloroform layer was washed with sodium bicarbonate twice, dried, and evaporated. NMR of the extremely viscous material (protonated trial) was identical to the spectrum of the purchased product. NMR of the deuterated compound showed similar shifts in the  $\beta$ -carbon as well as the amide proton (vb 5.8 ppm). Sublimation three times produced the pure material. The overall yield was 50%.

**NMR Measurements.** Spectra were collected on a Chemagnetics CMX400 equipped with a broad-line deuterium probe and a 7 mm CPMAS probe. The deuterium line shapes were collected with a standard quadrupolar echo sequence. The anisotropy experiments were collected with an inversion pulse followed by a variable delay time and detected with the quadrupolar echo sequence. The  $\pi/2$  pulse length was set to 2.0  $\mu$ s, and the FID was sampled at 2 MHz with a total length of 1024 complex points. The relaxation delay was approximately 5 $T_1$  for each sample (varying from 3 to 600 s). All spectra were processed with 2 kHz of line broadening with the exception of the variable-temperature line shape study, wherein subtle changes in line shapes were studied without line

**TABLE 1: Deuterium Spin–Lattice Relaxation Data and the  $^{13}\text{C}$  CSA Values**

compound	$^2\text{H } T_1$ (s)	$e\text{EqQ}$ (kHz)	$\eta$	$\delta_{11}$ (ppm)	$\delta_{22}$ (ppm)	$\delta_{33}$ (ppm)
(1) acetamide	115	197	0.12	88	197	246
(2) urea	50	211	0.11			
(3) caprolactam	64	177	0.16	97	200	249
(4) glycine anhydride	290			82	182	244
(5) homoazaadamantone	>200	210	0.18	102	189	242
(6) 2-pyridone	>300			84	172	237
(7) acetanilide	>300	189	0.19	90	175	248
(8) benzanilide	>600					
(9) caprylolactam	1.2	194	0.16	95	193	249
(10) caprylolactam·HCl	1.2			82	201	262
(11) cyclic monomer N-6,6	1.5	203	0.17	90	190	238
(12) <i>N,N'</i> -heptamethylenedibenzamide	45					
(13) <i>N,N'</i> -hexamethylenediacetamide	172			85	181	237
(14) <i>N,N'</i> -hexamethylenedibenzamide	>300					
(15) <i>N,N'</i> -hexamethylenedipropionamide	166			100	186	240
(16) <i>N</i> -methylbenzamide	288					
(17) <i>N,N'</i> -octamethylenedibenzamide	>300					
(18) polyalanine	1.0			95	178	243
(19) polyamide 4,6	4.3			92	189	243
(20) <i>N</i> - <i>tert</i> -butylpropamide	~7	193	0.134	94	183	250
(21) <i>N</i> -(1-adamantyl)acetamide	27			94	174	246
(22) lauryllactam	0.43	205	0.154	92	181	246
(23) <i>N,N'</i> -hexamethylenedi-hexamide	144			88	184	248
(24) <i>N</i> - <i>tert</i> -butylacetamide				93	175	245
(25) <i>N,N'</i> -di- <i>n</i> -butyladipamide	1.4			88	183	249
(26) <i>N,N'</i> -diisopropyladipamide	7.2	179	0.136	96	183	244
(27) <i>N,N'</i> -tetramethylenedi-butylamide	3.5			86	174	243
(28) <i>N</i> -acetyl-glycine	100					
(29) polybenzyl glutamate	1.0					

broadening.  $T_1$  values reported in Table 1 were obtained by fitting the integrated intensity of the Fourier transform of the FID to  $I(t) = I_0(1 - 2 \exp[-t/T_1])$ .

The  $^{13}\text{C}$  CPMAS spectra were collected with decoupling powers over 50 kHz and contact times of 3 ms. Spectra from three spinning speeds were used to determine the isotropic shift and to estimate the error in the CSA measurements. The tensor elements were extracted by Herzfeld–Berger analysis.<sup>22</sup>

## Results and Discussion

**Correlation of  $^2\text{H } T_{1Z}$  and Structure.** We have measured the deuterium spin–lattice relaxation rates of approximately 25 amides, which range from less than 1 s to more than 600 s (Table 1) most of which have been characterized by X-ray crystallography (Table 2). Although anisotropic relaxation is an especially useful method in discriminating different dynamical models (*vide infra*), we report the relaxation times based upon the intensity of the first point of the FID (related to the integrated intensity of the spectrum) for many of these compounds because of their long spin–lattice relaxation times and associated poor signal-to-noise ratios. In order to analyze the variation in the deuterium relaxation rates of these crystalline amides, we selected amides that vary in intramolecular conformation, hydrogen bond geometry, crystalline packing arrangement, and side chain moiety.

In studying the correlation between structure and relaxation rate, we are making an implicit assumption that the motion that drives relaxation is common throughout the database. The relaxation mechanism is common among all of the samples studied, to the extent that all of the cases with efficient relaxation are driven by a librational process. On the other hand, the motion varies from one compound to another in terms of the extent of anisotropy; in other words, some compounds relax through purely out-of-plane libration, while others enact a more isotropic motion such as “wobbling in a cone” or “wobbling on the surface of a cone”, as evidenced by their  $T_1$  anisotropy

spectra (*vide infra*). Furthermore, we do not know the extent to which the principal normal mode for the motion involves flanking alkyl groups or neighboring molecules; this extent could vary from one rapidly relaxing compound to another. Nonetheless, we looked for correlations between  $T_1$  and structure; the interpretation of any correlation that we find has an implicit assumption of an essentially common relaxation mode.

Several general observations can be made about the structures and packing of the amides. Amide hydrogen bond donors and acceptors are invariably satisfied in crystalline structures.<sup>23–27</sup> The hydrogen bond length varies over the range 2.7–3.1 Å ( $\text{NH}\cdots\text{O}=\text{C}$ ), and the angle ( $\text{NH}\cdots\text{O}=\text{C}$ ) is more widely variable (110–180°). A study of over 1400  $\text{CO}\cdots\text{HN}$  hydrogen bonds characterized by X-ray crystallography as well as several by neutron diffraction did not find a strong preference in the intermolecular  $\text{NH}\cdots\text{OC}$  bond angle.<sup>27</sup> Probably the reason for the variation and weak preference is that the hydrogen bond geometry is dictated by other considerations. There are distinct geometries that are known for cis and trans amides (Figure 1).<sup>24</sup> Cis amides often pack as cyclic dimers, and then these dimers are propagated by a translation element to complete the crystal (e.g., caprolactam) or utilize a local 2-fold screw element, which results in an infinite helix (e.g.,  $\alpha$ -pyridone) (Figure 1). In this case the  $\text{NH}\cdots\text{OC}$  bond angles are typically 120°. This packing arrangement is impossible for trans amides. For trans amides, the amide often packs using a simple translation (e.g., caprylolactam (Figure 1) or a 2-fold glide (e.g., *N*-methylbenzamide) (Figure 1); the  $\text{NH}\cdots\text{OC}$  bond angle is generally 140–180°. The side chains for cis amides prohibit the formation of a packing arrangement with a simple 2-fold glide. We use these motif designations to describe the amides in this study; however no relation between packing and relaxation behavior was seen.

The only correlation we have detected between the amide deuterium relaxation rate ( $^2\text{H } T_{1Z}$ ) and the structure of the compound involves the alkyl groups adjacent to the amide. Only amides with flanking alkyl groups larger than a methyl group

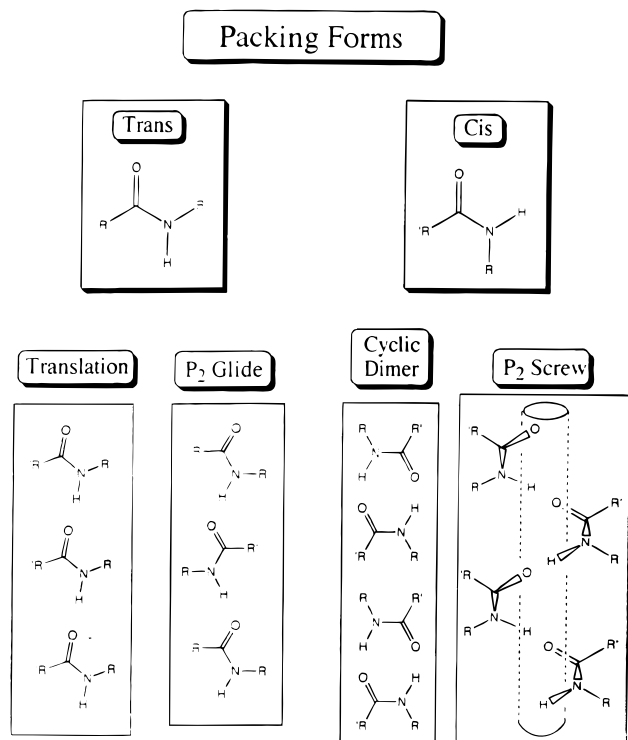


**Figure 1.** Different packing forms common for cis and trans amides, including the compounds used in this study. Each packing form places geometric restrictions on the hydrogen bond.

exhibit librational dynamics on the NMR time scale. Furthermore there is a rough relation between the dihedral angles in these flanking groups and the presence of "slow" librational dynamics. A  $\phi/\psi$  map similar to those used to describe peptide conformation (Ramachandran plot) is shown in Figure 2. (Note that unlike the conventional plot used to describe protein structure we are plotting the two angles flanking an individual amide.) Compounds with a conformation near  $\phi = -60^\circ$  and  $\psi = -60^\circ$  include caprylolactam, polyamide-4,6, the cyclic monomer, polyalanine, and PBG; these compounds all have fast  $^2\text{H } T_{1\rho}$  values (Table 2). The 2D map exhibits an "island" of fast relaxing amides. Compounds with this conformation are also characterized by gauche eclipsing interactions between the amide and the protons of the flanking methylene. For the polyamide-4,6, the cyclic monomer, and caprylolactam the formation of the ring forces the adjacent methylene groups to take on a gauche conformation. In the case of polyalanine and PBG, the formation of the hydrogen bond to the  $i+4$  and  $i-4$  amides necessitates these dihedral angles. For acyclic amides such as hexamethylene dibenzamide this restriction is lifted and the methylene chain can take on an all-trans conformation.

Several of the compounds that are not displayed on the  $\phi/\psi$  map are branched at the methylene group such that the dihedral angle is not well-defined. For instance, *tert*-butylpropionamide, which has a "medium" value  $T_1$  of 7.2 s, cannot be defined since the group adjacent to the amide nitrogen is a tertiary butyl group. The other dihedral,  $\text{NC(=O)-CC}$ , is  $-147^\circ$ , which is similar to the fast relaxing amides. Dihedral angles for others such as *N*-methylbenzamide or hexamethylenediacetamide cannot be defined since no fourth main chain atom exists (e.g.  $\text{NHC(=O)CH}_3$ ); as mentioned above, these compounds, with only a methyl group on one side, exhibit a long relaxation time. Some amides in our study that lack crystallographic characterization also have a short relaxation time. The spin-lattice relaxation times for *N,N'*-di-*n*-butyladipamide, *N,N'*-di-*n*-pro-

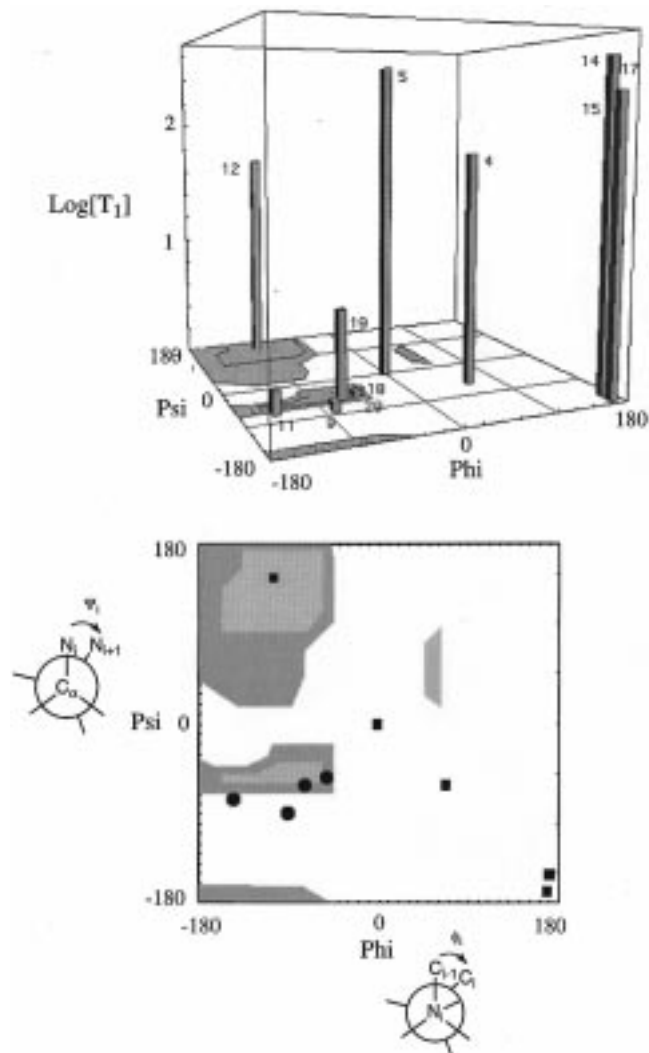


**Figure 2.** (top)  $\phi/\psi$  angles plotted as a function of the logarithm of deuterium longitudinal relaxation time. The numbers adjacent to the boxes refer to the compound given in Table 2. The points with short spin-lattice relaxation times are clustered about  $\phi/\psi$  angles of an  $\alpha$ -helix,  $\{-60^\circ, -60^\circ\}$ . Some of the amides with long spin-lattice relaxation times occupy regions of  $\phi/\psi$  that are normally inaccessible for peptides with the exception of point 12, which occupies the region assigned to the  $\beta$ -sheet. (bottom) Projection of the values onto the  $\phi/\psi$  plane: the solid circles represent compounds with a relaxation time less than 5 s (most  $\sim 1$  s), and the solid squares represent compounds with a relaxation time longer than 50 s (most of which are greater than 100 s). This figure represents the definition of the Ramachandran angles used in this study and typically used to describe the secondary structure of peptides.

pyladipamide, and nylon-4,4 are 1.4, 7.2, and 1 s, respectively. The crystal structure of a similar compound, *N,N'*-diethyladipamide, shows that the dihedral angle adjacent to the carbonyl is also gauche;<sup>28</sup> if our compounds pack in the same manner, they would agree with the proposed trend between dihedral angles and relaxation times. Nylon 66 exhibits a short spin-lattice relaxation for both the methylene and the amide<sup>29</sup> and has flanking dihedral angles in an all-trans conformation. This compound would break the general rule we are proposing about the relation between flanking dihedral angles and relaxation rate, unless gauche defects occur in large population near the phase transition. We report herein data on a compound similar to nylon 66, *N,N'*-hexamethylenhexamide, but with the amides reversed {e.g.  $\text{C(=O)N}$  vs  $\text{NC(=O)}$ }, which has a long spin-lattice relaxation rate.

TABLE 2: Crystallographic Information for the Compounds Used in This Study

compound	$\angle\text{NOC}$	N $\cdots$ O	IR bands		torsional angles			packing	ref
			CO	NH	CCNC $\psi$	CNCC $\omega$	NCCC $\phi$		
(1) acetamide	121/120	2.99	1607					3D array	[Hamilton, 1965]
(2) urea	147/167	3.02						3D array	[Donahue, 1940]
(3) caprolactam	121	2.90	1656	3223	67.8	-4.1	-63.2	cyclic	[Winkler, 1975a]
(4) glycine anhydride	122	2.85	1705	3193	-1.3	1.3	-1.2	cyclic	[Degeilh, 1959]
(5) homoazaadamantone	119	2.90	1657	3196		-3.5		cyclic	[Symersky, 1986]
(6) 2-pyridone	136	2.77	1639		0	-1	0	P <sub>2</sub> screw	[Penfold, 1953]
(7) acetanilide	139	2.94	1642	3298	-160	177		P <sub>2</sub> screw	[Brown, 1966]
(8) benzanilide	161	3.11	1646	3347	-31.3	$\sim$ 180	31.6	P <sub>2</sub> screw	[Kashino, 1979]
(9) caprylolactam	174	2.86	1634	3319	-90.4	148.4	-88.8	trans	[Winkler, 1975b]
(10) caprylolactam $\cdot$ HCl			1685		86.6	-171.4	-101.1	P <sub>2</sub> screw	[Winkler, 1975b]
(11) cyclic monomer N-6,6	140	2.88	1633	1634	-145.3	175.5	75.3	P <sub>2</sub> screw	[Northolt, 1968]
(12) <i>N,N'</i> -heptamethylenedibenzamide	151	2.88	3323	1628	92.6	172.2	155.4	P <sub>2</sub> glide	[Brisson, 1982]
					-105.1	-172.2	145.8		
(13) <i>N,N'</i> -hexamethylenediacetamide	175	2.88	1625	3309	-168.1	-178.6		trans	[Bailey, 1955]
(14) <i>N,N'</i> -hexamethylenedibenzamide	165	3.01	1630	3322	171.2	-178.9	-152.5	trans	[Pineault, 1983]
(15) <i>N,N'</i> -hexamethylenedipropionamide	174	2.95	1634	3312	168.6	-176.9	-169.5	P <sub>2</sub> glide	[Jensen, 1957]
(16) <i>N</i> -methylbenzamide	140	2.92	1631	3333		179.1	-14.3	P <sub>2</sub> glide	[Leisoriwitz, 1978]
(17) <i>N,N'</i> -octamethylenedibenzamide	164	3.01			-170.9	179.1	-152.5	trans	[Pineault, 1983b]
(18) polyalanine	164	2.86	1645	3282	-57.	179.	-54.		[Arnott, 1966]
(19) polyamide 4,6	167	2.87	1630	3311	-74.	167.1	-60.8		[Vulić, 1994]
(20) <i>N-tert</i> -butylpropionamide	160	2.98	1646	3319	-147	-174			[this study]
(21) <i>N</i> -(1-adamantyl)acetamide			1636	3324					
(22) lauryllactam			1641	3310					
(23) <i>N,N'</i> -hexamethylenedihexamide			1634	3306					
(24) <i>N-tert</i> -butylacetamide			1648	3290					
			1669						
(25) <i>N,N'</i> -di- <i>n</i> -butyladipamide	trans		1626	3303					
(26) <i>N,N'</i> -diisopropyladipamide	trans		1638	3306					
(27) <i>N,N'</i> -tetramethylenedibutylamide									

In order to study the effect of the alkyl group, a homologous series with the same packing arrangement was studied: hexamethylenediacetamide, hexamethylenedipropionamide, hexamethylenedihexamide, and hexamethylenedibenzamide {RC(=O)NH(CH<sub>2</sub>)<sub>6</sub>NHC(=O)-R, where R = methyl, ethyl, hexamethyl, phenyl groups}. All of these compounds exhibit long relaxation rates. In another series of compounds with similar packing the alkyl groups vary enormously, but the relaxation rates are consistently very long: R-C(=O)NH-R': acetanilide, where R = methyl group and R' = phenyl group; *N*-methylbenzamide, where R = phenyl group and R' = methyl group; and benzanilide, where R = R' = phenyl group.

Strain incurred by closing the ring in lactams causes the amide unit to become nonplanar. We considered the possibility that such a strain would cause variation in the electronic structure and therefore a variation in conformational dynamics. This deviation is expressed in terms of a dihedral angle,  $\omega = \text{CN}-\text{C}(=\text{O})\text{C}$ , where values are either greater than 0° for cis amides or less than 180° for trans amides.<sup>30</sup> The deformation defined here is the magnitude from either trans,  $|\omega_d| = |180 - \omega|$ , or cis,  $|\omega_d| = |0 - \omega|$ . For caprylolactam this deformation is considerable,  $|\omega_d| = 33^\circ$ , a particularly large deviation. (This correlation is available in the Supporting Information, Figure 1.) Although there is a somewhat greater range in nonplanar distortion for the amides with a fast deuterium  $T_1$  as compared to the amides with a slow deuterium  $T_1$ , the correlation is unconvincing.

From the data compiled in Tables 1 and 2, we can rule out other structural properties as determining the deuterium relaxation rates and associated dynamics: there is no correlation between the deuterium relaxation rate and the amide conformation (cis vs trans), nor for hydrogen bond length, hydrogen bond angle, or packing form. Typically the trans amides relax faster than the cis amides; however, there are exceptions (e.g., hexamethylenediacetamide, a trans amide with a spin-lattice

relaxation time of 167 s). The packing arrangement fails to correlate with the deuterium relaxation rates. (See Figure 4-3 of ref 56.) The density and the Debye-Waller thermal factors (data not shown) derived from the crystal structure also did not correlate with the relaxation rates.

**Chemical Shift Tensors, QCC, and IR.** Hydrogen bonding can have a dramatic effect on the electronic structure of the hydrogen bond donor and acceptor. This is evidenced by band shifts in IR frequencies, changes in UV-vis absorption, and NMR chemical shifts. To test whether the variable dynamics responsible for the variable deuterium relaxation times are associated with changes in electronic structures of the amides, we have measured the <sup>13</sup>C chemical shift anisotropy of the carbonyl, the IR spectra, and the quadrupolar coupling constant (QCC) of most of these amides, and we have compared these spectroscopic signatures to the structures as well as to the relaxation rates. In response to hydrogen-bonding interactions, the oxygen of an amide group purportedly becomes more negatively charged and the CN bond more double bond-like; these features have been invoked to explain the trends in IR spectra, NMR spectra, X-ray lengths, and cis-trans rotation barriers. This hypothesis, however, is not borne out by our data. Infrared spectra for each compound offer evidence that the resonance structures are not substantially variable for most of the secondary compounds and are not strongly affected by ring strain. The NH stretch and the amide I stretch (mostly associated with the carbonyl) are reported in Table 2. The average value of the carbonyl frequency is  $\sim 1645 \pm 23 \text{ cm}^{-1}$ , and the NH stretch is  $3254 \pm 80 \text{ cm}^{-1}$ , with no significant correlation with the ring strain (data not shown). IR bond stretches were compared to the CO, CN, and N $\cdots$ O bond lengths, revealing no correlation. The correlation between the intermolecular N $\cdots$ O bond length and the CO bond length or between the CN bond length and the CO bond length was also weak (see Figure 4-11 of ref 56).

The chemical tensor elements of the amide carbonyl are shown in Figure 3;  $\delta_{22}$  is along the C=O bond direction,  $\delta_{33}$  is out of the amide plane, and  $\delta_{11}$  is normal to both and in-plane, approximately  $30^\circ$  to the CN bond.<sup>31</sup> Asakawa *et al.* have measured the chemical shift tensors for six alanine-containing peptides and calculated the tensor for canonical peptide conformations, the  $\beta$ -sheet, and  $\alpha$ -helix.<sup>32</sup> As the hydrogen bond length,  $R_{N\cdots O}$ , increases, the  $\delta_{33}$  element shifts downfield and the  $\delta_{22}$  element shifts upfield, but little change in the  $\delta_{11}$  element was reported, both for experimental and calculated shifts. In contrast, previous solid state NMR studies of the carboxyl group<sup>33</sup> show that the principal elements of the chemical shift tensor,  $\delta_{11}$ ,  $\delta_{22}$ , and  $\delta_{33}$ , are very sensitive to the length and (in the case of carboxylic acids) the geometry of the hydrogen bond. In the carboxylic acid study,  $\delta_{11}$  showed little variation, whereas  $\delta_{33}$  correlated well with whether the carboxyl group was protonated or deprotonated and  $\delta_{22}$  correlated well with the hydrogen bond strength.

The tensor elements for the amides reported herein are given in Table 1 and are within the range previously reported in the literature. Several of the tensors were not measured due to prohibitively long proton relaxation (which affects the rate of data acquisition for CPMAS studies). It is interesting that the proton relaxation times reflected the same trend observed for the deuterium  $T_1$ , despite the presence of methyl groups in some (such as *N*-methylbenzamide, which had a proton  $T_1$  on the order of 2 min). Spin–lattice relaxation rates for the protons, however, were not quantitatively measured in general and are not reported.

In our database, the  $^{13}\text{C}$  CSA were only poorly correlated with the bond lengths and other measures of the hydrogen bond; the hydrogen bond strength in this series of compounds is probably not variable enough to show the trends clearly. In particular, no correlation was observed between the  $^{13}\text{C}$  CSA tensor elements and the  $\text{NH}\cdots\text{OC}$  bond angle or  $\text{N}\cdots\text{O}$  bond length nor with the out-of-phase deformation caused by ring strain. Furthermore, there is none between the deuterium  $T_1$  and the chemical shift elements (data not shown). Moreover, there is no correlation between the chemical shift tensor elements and the infrared frequencies. (See Figure 4–10 of ref 56.) There is, however, a previously unreported correlation between  $\delta_{22}$  and  $\delta_{33}$  and the dihedral angle  $\psi$  which might be relevant for protein studies.

The modest variation of the  $^{13}\text{C}$  CSA elements in response to structural properties may be due to the limited hydrogen bond range,  $\sim 2.7$  to  $2.9$  Å. The limited range has been noted previously; a study of the Coulombic force associated with each of these different packing and hydrogen bond geometries indicate that the contribution of the Coulomb energy to the hydrogen bond strength is not strongly affected by modest changes in the length or the angle.<sup>25</sup> It has also been shown that the low-field shift in  $^{13}\text{C}$  solution NMR spectra due to carbonyl protonation is compensated by the upfield shift due to the formation of NH hydrogen bond.<sup>34</sup> Such a compensation may be responsible for the lack of variation in the chemical shift tensor elements for weak hydrogen bonds. A detailed comparison of the chemical shift tensors for  $^{15}\text{N}$  and  $^{13}\text{C}$  of acetanilide (which forms hydrogen bonds) and *N*-methylacetanilide (which cannot form hydrogen bonds) also showed little differences in the tensor elements of the carbonyl carbon ( $\delta_{11} = 248$  vs  $243$ ,  $\delta_{22} = 175$  and  $175$ , and  $\delta_{33} = 90$  vs  $93$  ppm, respectively).<sup>35</sup>

A substantial change in the tensor elements was observed for the HCl salt of caprylolactam. A downfield shift was seen

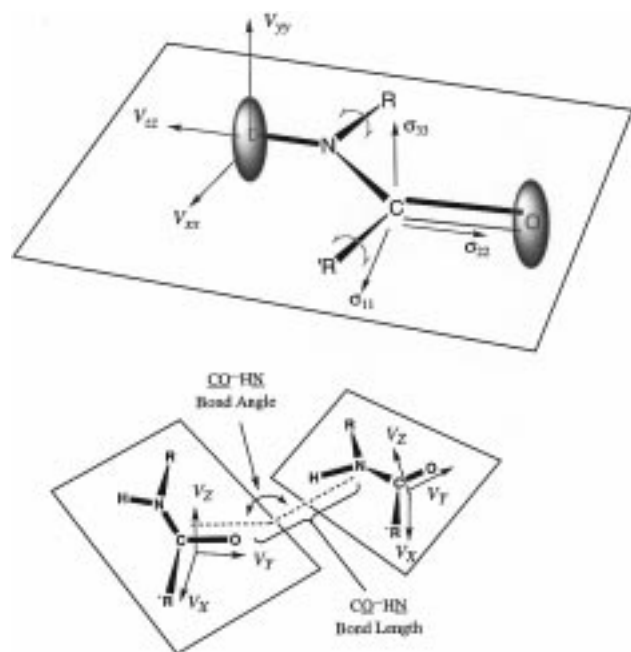
in the  $\delta_{11}$  and  $\delta_{22}$  elements when compared to the neutral compound. These changes are most likely due to the protonation of the carbonyl. Acetamide also exhibits a relatively downfield  $\delta_{22}$  shift and has two hydrogen bonds for the carbonyl (whereas most accept only one). Considerable changes in the CN and CO bond lengths are observed for the neutral and the HCl form of caprylolactam. The average bond lengths for the CN and CO bonds for all compounds in this study are  $1.247$  Å ( $\pm 0.022$ ) and  $1.338$  Å ( $\pm 0.015$ ). The CN and CO bond lengths are  $1.34$  and  $1.24$  Å for caprylolactam and  $1.31$  and  $1.30$  Å for the HCl salt of caprylolactam, respectively;<sup>36</sup> a  $7^\circ$  change in the O–C–N bond angle is also seen from the two compounds. Thus, the spectroscopic indicators certainly are sensitive to these more dramatic geometric changes upon full protonation, but the effects of weak hydrogen bonding are apparently masked by other environmental and internal variations in the compounds.

The quadrupolar coupling constant,  $\text{QCC} = e^2qQ/h$ , and its anisotropy,  $\eta$ , were also measured. These values probe the electric field gradient experienced at the deuterium nucleus and are sensitive indicators of the hydrogen bond strength. An empirical relation shows that the coupling is related to the  $\text{ND}\cdots\text{O}$  distance by  $\text{QCC} = A - B/r^3$ , where  $A = 282$  and  $B = -572$  and  $r$  is the distance between the deuterium and oxygen.<sup>18</sup> The values for both the coupling constant and the quadrupolar anisotropy are presented in Table 1. The quadrupolar coupling constants that were measured showed a modest variation, as expected (data not shown). However, none of the crystal structures of the amides in our study was solved using neutron methods, so the lengths of the NH distance as well as the  $\text{H}\cdots\text{O}$  distance were not amenable to detailed analyses.

These measurements indicate that the carbonyl CSA, IR, and quadrupolar coupling constants for secondary amides vary only to a subtle extent, and presumably the electronic structure varies rather little as well, with the exception of the HCl salt. A much more dramatic trend in chemical shift tensor elements for carboxyl groups has been observed previously in response to hydrogen bonding. Our conclusion is that the variation in librational dynamics is unlikely to result from variation in electronic properties associated with hydrogen bonding.

**Librational Dynamics.** We present a model for the type of motion responsible for the relaxation based upon our data and previous discussion in the literature. Some characteristics of the motion are directly available from the data, for example the direction of the libration, the approximate angle, and the fact that it is not an activated process, and these characteristics will be discussed first. To obtain other characteristics such as the effective correlation time, we must assume a model for the motion. Models for librational dynamics and typical time scales are discussed in the following section, based upon previous literature. Finally, we offer an interpretation for the connection between the flanking alkyl groups and the librational characteristics.

The direction of the libration and the approximate excursion angle are two characteristics directly available from the data. The singularities observed in a static deuterium spectrum correspond to deuterium at specific angles with respect to the applied field; changes in the positions of these singularities with temperature are indicative of the type of molecular motion experienced by the deuterium (Figure 4). Single-crystal studies of urea and *N*-acetyl glycine have shown that the  $V_{zz}$  component is along the N–D bond, the  $V_{yy}$  component is normal to the amide plane, and the  $V_{xx}$  is in the amide plane, perpendicular to the remaining components.<sup>37,38</sup> All amides in this study



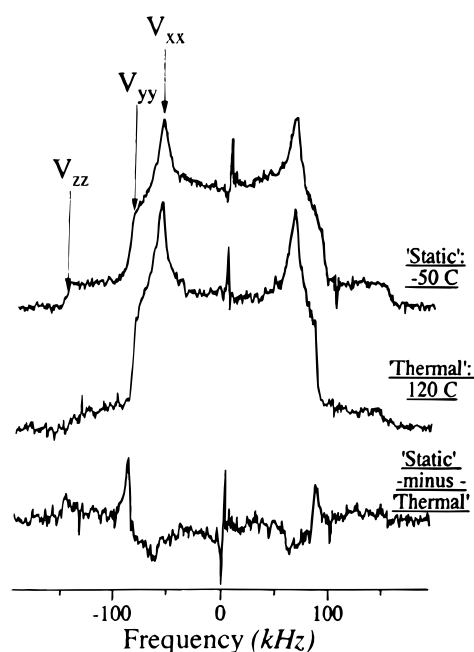
**Figure 3.** (a) Components of the deuteron electric field gradient ( $V_{xx}$ ,  $V_{yy}$ ,  $V_{zz}$ ) and carbonyl chemical shift anisotropy ( $\sigma_{11}$ ,  $\sigma_{22}$ ,  $\sigma_{33}$ ) drawn onto the molecular geometry of a trans amide. Both components  $V_{yy}$  and  $\sigma_{22}$  are normal to the amide plane. Note that the motion observed for several of the fast relaxing amides modulates the  $V_{yy}$  and  $V_{zz}$  components as indicated by the ellipsoid. (b) The  $NH\cdots OC$  bond length, the  $NH\cdots OC$  bond angle, and a Cartesian coordinate system used to relate neighboring amides via Euler angles.

exhibit approximately static N–D deuterium line shapes, which eliminates the possibility of large-amplitude molecular motions.

Temperature-dependent line shapes of the fast relaxing amides indicate that the motion responsible for the relaxation is an out-of-plane libration. Detailed studies from other labs have also described an out-of-plane libration for the amide unit in polybenzyl glutamate<sup>38</sup> and nylon 66.<sup>29</sup> Following the example of the study of Usha *et al.*,<sup>38</sup> we measured the line shape of a short amide, lauryllactam, at 223 and 393 K (Figure 4). The subtracted spectra (corresponding to the two temperatures) show differences, especially at 87 kHz corresponding to the  $V_{yy}$  direction of the electric field gradient at the deuteron. This residual intensity can be related to the difference in the root mean square of the polar angles,  $\theta$  and  $\phi$ , at different temperatures.<sup>39</sup> The reduction of the spectral intensity at the y-component is consistent with an out-of-plane libration which increases its angular excursion with an increase in temperature, which can be described by  $\delta\theta \cong \sin^{-1}(\delta\omega/(2\eta e^2 q Q/h))$ . The quadrupolar coupling constant of lauryllactam at 223 K is 195 kHz, its anisotropy is 0.17, and the fwhm of the residual spectral density is 5 kHz; therefore the increase in angular excursion is  $4.3^\circ$  over 150 K, or 0.025 deg/K. This value is similar to that reported for polybenzyl glutamate, which increased its angular excursion linearly from  $8^\circ$  at 200 K to  $12^\circ$  at 400 K.<sup>38</sup>

Detailed studies of the thermal parameters from diffraction data for glycine anhydride<sup>40</sup> and urea<sup>41</sup> indicate that the amplitude of the out-of-plane libration can be as much as  $8$ – $12^\circ$ , similar to that estimated from deuterium line-shape analysis for caprylolactam in our study, and to the values estimated for PBG<sup>38</sup> and nylon 66.<sup>29</sup> Thus similar thermal factors in the diffraction data are indicated for compounds with short and long  $T_1$  deuterium values.

The direction of motion can also be probed with anisotropic relaxation measurements. Two  $T_1$  anisotropy spectra of capry-



**Figure 4.** Line shapes of lauryllactam taken at  $-50$  and  $120^\circ\text{C}$  and the difference (scaled by the Boltzmann factor). The singularities are marked  $V_{xx}$ ,  $V_{yy}$ ,  $V_{zz}$ , corresponding to the principle axes the quadrupole tensor. The singularity labeled  $V_{zz}$  corresponds to all amides with N–D bonds aligned along the applied field. The singularity labeled  $V_{xx}$  corresponds to all amides with N–D bonds and vectors normal to the amide plane perpendicular to the applied field. Finally, the component marked  $V_{yy}$  corresponds to all amides both with the N–D bonds perpendicular to the applied field and with vectors normal of the amide plane parallel to the applied field. The spectral intensity in the difference spectra is mostly associated with the y-component of the electric field gradient and indicates an out-of-plane libration. By increasing the temperature, the angular excursion for the out-of-plane libration is increased. The full width at half-maximum of the remaining spectral intensity in the difference spectra is 5 kHz, which corresponds to an increase of approximately  $4.3^\circ$  in angular excursion between the two temperatures.

lolactam are shown in Figure 5: one with a delay near the  $T_1$  zero-crossing and the other with a delay of 5 times the spin–lattice relaxation time. The principal tensor elements corresponding to the direction of the N–D bond vector are indicated on the spectrum. It is clear that the z-component and the y-component are fully relaxed at the zero crossing, whereas the x-components are still inverted. Molecular motion produces spectra density at the Larmor frequency and twice the Larmor frequency of the deuteron (61 and 122 MHz at 9.4 T, respectively) most efficiently when the amides are aligned with their z and y tensor components along the applied field.  $T_1$  is given by

$$\frac{1}{T_1}(\Omega_{\text{PL}}) = \frac{3}{8} \left( \frac{eqEQ}{\hbar} \right)^2 [J_1(\Omega', \omega) + 4J_2(\Omega', 2\omega)] \quad (1)$$

where  $J_m(\Omega_{\text{PL}}, \omega)$ , the spectral density at frequency  $\omega$  for a molecule at an orientation  $\Omega_{\text{PL}}$  with respect to the applied field, is

$$J_m(\Omega_{\text{PL}}, \omega) = \int_0^\infty C_m(\Omega', t) \cos(\omega t) dt \quad (2)$$

and  $C_m(\Omega_{\text{PL}}, t)$  is the correlation function for the motion,

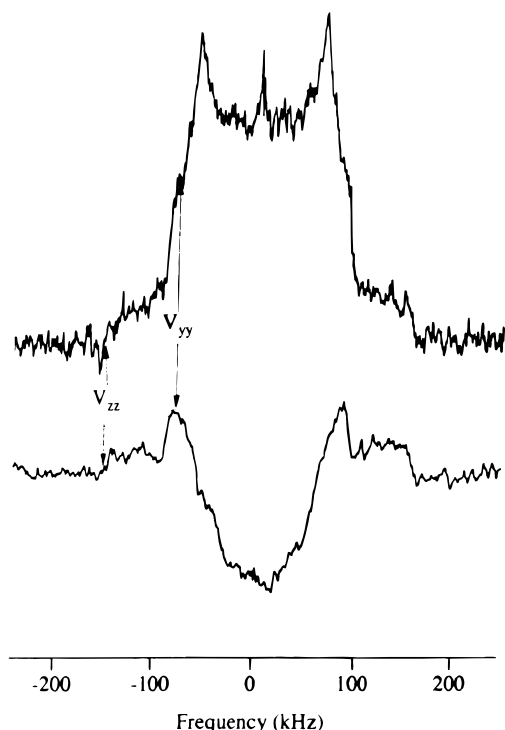


**Figure 5.** Anisotropy spectra of deuterium-exchanged caprylolactam collected with the relaxation delay set to the “zero-crossing” time and at 8 times the spin–lattice relaxation time (spectra collected at room temperature). Note that the wings at  $\pm 145$  kHz (marked  $V_{zz}$ ) and the shoulders at  $\pm 86$  kHz (marked  $V_{yy}$ ) are fully relaxed at a 1.0 s delay, whereas the horns at  $\pm 63$  kHz (marked  $V_{xx}$ ) are still mostly inverted. The rate of relaxation is determined by molecular motion at  $1\times$  and  $2\times$  Larmor frequency (60.8 and 121.6 MHz) and is dependent on the polar angles  $\theta$  and  $\phi$ . The observed anisotropy in the relaxation rate indicates that the  $V_{yy}$  and  $V_{zz}$  components are more effectively modulated than the  $V_{xx}$  component. This observation is also consistent with an out-of-plane libration which pivots about the  $V_{xx}$  component.

$$C_m(\Omega_{PL}, t) = (\rho_{20})^{-2} \sum_{\substack{mm'=-2 \\ aa'=-2}}^2 \rho_{2m}\rho_{2m'} D_{am}^{(2)*}(\Omega_{CL}) D_{a'm}^{(2)}(\Omega_{CL}) \langle D_{an}^{(2)*}(\Omega_{PC}(0)) D_{a'n}^{(2)}(\Omega_{PC}(t)) \rangle \quad (3)$$

$D_{am}^{(2)*}(\Omega)$  is the Wigner rotation matrix,  $\Omega$  represents the set of Euler angles that transform one frame to another frame, and  $\rho_{20}$  is the strength of the quadrupolar interaction ( $\sqrt{2/3}eq$ ).<sup>13</sup> The correlation function contains a time-dependent term that describes the motion in a molecular fixed frame (the bracketed term). The time-dependent Euler angles,  $\Omega_{PC}(t)$ , describe the motion in terms of the coordinate system of the molecule; these angles rotate the principal axis system of the molecule to a crystal fixed frame, and the crystal fixed frame is assumed to be time independent. (For the principal axis system, the direction from the N–D vector is the  $z$ -axis, and the vector in the amide plane orthogonal to  $z$  is the  $x$ -axis.) The Euler angles,  $\Omega_{CL}$ , which are time independent (nonbracketed term), rotate the molecular fixed frame into the laboratory frame. If the motion is anisotropic such as an out-of-plane libration, then the correlation function, the spectral density, and the relaxation will be anisotropic as well and are explicit functions of the orientation of the amide with respect to the applied field.

Specific values of the anisotropic relaxation rates can be calculated given a model of the molecular motion. For example, we propose that the amide is executing an out-of-plane libration about an axis approximately aligned with the  $x$ -component of

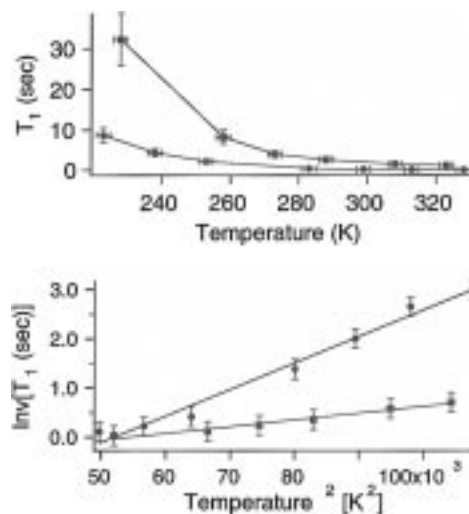


**Figure 6.** Spin–lattice relaxation for methylene- and nitrogen-deuterated caprylolactam as a function of temperature. The top graph is simply  $T_1$  vs temperature for both samples where the circles (lower curve) are for the  $\alpha$ -methylene and the squares (upper curve) are for N–D. The bottom graph is the inverse of the spin–lattice relaxation time as a function of temperature squared where the circles (upper curve) are for the  $\alpha$ -methylene and the squares (lower curve) are for N–D. The “slope” is proportional to the angular excursion, the quadrupolar coupling constant, and the diffusion constant (see text for further discussion). The errors for the temperature and rate are shown as 1% and 15% RSD, respectively, although the error in most measurements is much less.

the electric field gradient, which would produce substantially more modulation for the  $y$ - and  $z$ -components than for the  $x$ -component. Anisotropic relaxation has been observed for caprylolactam, for lauryllactam, for the cyclic monomer as well as for caprolactam near its melting point (55 °C); the extent of the anisotropy is quite modest for others which are considerably less crystalline, such as polyalanine. In the more amorphous materials it is possible that the model for the motion should be closer to random motion in a cone. Simulation of the out-of-plane rocking of the amide with a single correlation time does not produce the amplitude of anisotropy observed in the spectra for caprylolactam. To reproduce the spectra, we must use a more complicated model, including motions on a wide range of time scales (data forthcoming).

To clarify the nature of the motion, methylene units adjacent to the amide for caprolactam and caprylolactam were specifically deuterated ( $\alpha$ -D lactams), and the corresponding deuterium  $T_1$  times were measured. In both cases the relaxation times for the methylene-deuterated sample were shorter than the N-D deuterated samples; for N-D caprolactam the  $T_1$  is 64 s, for  $CD_2$ –CO–NH– $CD_2$  caprolactam the  $T_1$  is 45 s, for N-D caprylolactam the  $T_1$  is 1.2 s, and for  $CD_2$ –CO–NH– $CD_2$  caprylolactam the  $T_1$  is 0.7 s (all at room temperature).<sup>29</sup> Line shapes for the methylene-deuterated compounds also resemble static Pake patterns with QCC values of 170 kHz. Anisotropic zero-crossing spectra of  $\alpha$ -D caprylolactam exhibited  $V_{zz}$  components that relax faster than the unresolved  $V_{xx}$  and  $V_{yy}$  components. Carbon relaxation measurements showed similar relaxation times for all methylenes, consistent with the proposal that the entire molecule librates with a similar time scale and angular extent.

The temperature dependence of the deuterium  $T_1$  relaxation rates for N–D and  $\alpha$ -D caprylolactam was measured. In Figure 6,  $T_1$  values are plotted as a function of temperature. The  $T_1$  for both N–D and  $\alpha$ -D decrease monotonically with temper-

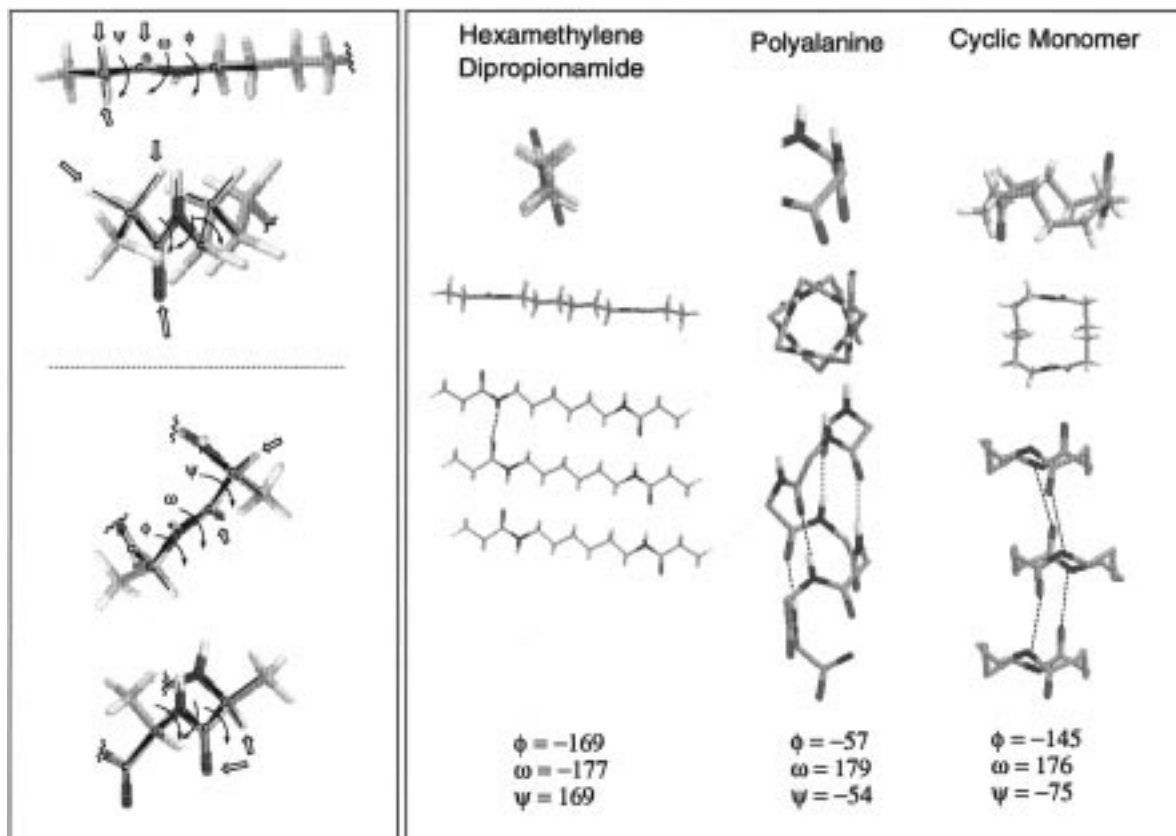


**Figure 7.** (left) Torsional angles,  $\phi$ ,  $\psi$ , and  $\tau$  represented as arrows drawn onto hexamethylenedipropionamide and polyalanine. Note that in the case of an  $\alpha$ -helix the proton on the carbon alpha to the CO eclipses oxygen and the proton alpha to the NH is in a gauche conformation. In the case of the hexamethylenedipropionamide the protons adjacent to both groups are in an all-trans conformation. The dihedral angles,  $\phi = C_2'C_1' - NC(=O)$ ,  $C_1'N - C(=O)C_1$ ,  $N(O=)C - C_1C_2$ , are defined in Figure 3. (right) Three views of the hexamethylenedipropionamide, two turns of polyalanine (without protons or the side chain), and the cyclic monomer. The top row is a projection down the molecular axis defined in Figure 3. The middle and bottom rows are projections down the  $y$ -axis and  $z$ -axis, respectively. For the cyclic monomer, the dihedral angles adjacent to the amide unit must take on a gauche conformation in order to complete the ring. For polyalanine in the  $\alpha$ -helix conformation the dihedrals after the amide unit are also gauche in order to satisfy hydrogen bonding with the  $i+4$  and  $i-4$  residue. For hexamethylenedipropionamide, there are no internal constraints and the methylene chain takes on an all-trans conformation.

ature. The relaxation times increase more slowly with decreasing temperature for the CD group compared to the N-D deuteron.

**Spectral Density and Librational Models.** In this section we discuss models relating the relaxation times to characteristic time constants for the libration. The models are derived largely from the literature. At the outset we were surprised to observe such short relaxation times associated with a librational motion. Typically, motions with large amplitudes with near equal populations between the sites and rates near the Larmor frequency (60.8 MHz) have fast relaxation rates (e.g., the methyl group three-site hop or a trans-gauche isomerization in lipid bilayers). An out-of-plane libration, as suggested by our data, is generally assumed to be of low amplitude and in the low IR/Raman frequency bands ( $10\text{--}50\text{ cm}^{-1}$  or  $47\text{--}238\text{ GHz}$ ). Thus, one might have expected all deuterated amides to have long deuterium  $T_1$  relaxation times. Nonetheless, small angular excursions have been proposed previously to explain small  $T_1$  values in other studies. Presumably, the reason that librations are able to act as a relaxation mechanism is that they become overdamped due to structural and conformational restraints. In this study, we use our structural survey together with previously published models to understand the molecular origin of this damping.

There are several previous examples for librational motions providing relaxation mechanisms. For example, a detailed relaxation study of *n*-nonadecane- $d_{40}$ /urea clathrate indicates that

the  $CD_2$  groups of the alkane chain undergo a small angle "wobble" of approximately  $20\text{--}30^\circ$  with the correlation time of  $10^{-10}\text{--}10^{-11}\text{ s}$ .<sup>42</sup> The deuterium relaxation data of cyclopentane- $d_{10}$  also indicate a small  $5\text{--}10^\circ$  libration that is quenched on passing from the phase II (a glassy state) to phase III (a crystalline state).<sup>43</sup> A small-angle libration of the tryptophan side chain in bacteriorhodopsin<sup>44</sup> and in triose phosphate isomerase<sup>45</sup> has been invoked to explain the fast relaxation rate.

The assumption that the principal contribution to the spectral density is on a time scale very fast compared to the Larmor frequency was confirmed by measuring the anisotropic relaxation of quadrupolar order.<sup>56</sup> For a fast-limit motion the relaxation times should follow the relation  $T_{1Q}/T_{1Z} = 5/3$ ; the rates were approximately in this ratio for the fast-relaxing amide caprylolactam HCl, and others are currently under investigation.

Theoretical treatments of the out-of-plane libration have been presented previously.<sup>31,38</sup> A model based on the stochastic diffusion equation has been shown to be essentially equivalent to a strongly damped Langevin oscillator with a harmonic driving force, where the motion is assumed to be on a fast time scale and involve small angle fluctuations; both models appear to explain the spin-lattice relaxation behavior.<sup>31,38,42,46</sup> A model based on the stochastic diffusion equation predicts a correlation time  $\tau(\Omega) \approx 12\langle\theta_{\text{lib}}^2(\Omega)\rangle/\pi^2D(\Omega)$  (eq 5) and an anisotropic (frequency-independent) spectral density  $J_m(\Omega) =$

$3/2\langle\theta_{\text{Lib}}^2\rangle\tau(\Omega)$  (eq 6)<sup>46</sup> where  $D(\Omega)$  is the (anisotropic) diffusion constant, the tensorial angular excursion  $\theta_{\text{Lib}}(\Omega)$  describes an oscillation which is primarily about the  $x$ -axis in the molecular frame, and  $\Omega$  represents the Euler angles which describe the orientation converting the principle axis system to the lab frame for each crystallite and must be used to compute the anisotropic parameters  $\Theta$ ,  $D$ , and  $\tau$ . An alternative model is based on a driven harmonic oscillator subject to friction.<sup>38,47,48</sup> The libration of the amide plane occurs along a coordinate,  $\eta$ , which is the difference of the Ramachandran angles,  $\eta = (\phi - \varphi)\sqrt{2}$ .<sup>38,49</sup> If this motion is subject to strong frictional damping with a damping constant  $\lambda$ , and the angular fluctuation is assumed to be small, it has been shown that the spectral density is  $J_m = 3\langle\theta_\eta^2\rangle(\lambda/\omega_\eta^2)$ <sup>38</sup> (eq 7), where the damping constant  $\lambda = \zeta/2I_\eta$ , the “undamped” frequency  $\omega_\eta = (\kappa T/I_\eta\langle\theta_\eta^2\rangle)^{1/2}$  (eq 8),  $I_\eta$  is the inertia,  $\kappa$  is the Boltzmann constant,  $T$  is the temperature, and  $\zeta$  is the friction coefficient.<sup>47</sup> Here the anisotropic spectral density and relaxation rates result from the fact that the normal mode must be projected onto the molecular axis system which in turn relates to the laboratory frame in a different way for each crystallite. The final expression for the spectral density for the Langevin oscillator model in the limit of strong friction can be compared with the one that results from the stochastic diffusion model using the Einstein relation,  $D = k_b T/\zeta$  (eq 9); the expressions differ then only by a small scaling constant. This similarity is interesting since the physical assumptions are very different; the spectral density of the damped Langevin oscillator would be centered about the oscillator frequency except that it extends to lower frequencies due to a frictional force, while the spectral density for the stochastic diffusion is inherently centered around zero frequency.<sup>38,48</sup> In the Langevin oscillator model, amides with long relaxation times would be described by weak frictional coefficients, so that the oscillator approaches the inertial limit and the spectral density is strongly peaked at the oscillator frequency.<sup>48</sup> Amides with short relaxation times would be described by strong frictional coefficients with “white” spectral density, which is analogous to the result derived from the stochastic diffusion model. In summary, we used previously derived theoretical models to recast our spin–lattice relaxation data in terms of a picture in which amides with certain conformations are usually subject to strong local frictional forces and librate diffusively and amides with other conformations are subject to weak local friction and librate harmonically, with rates far above the NMR time scale.

With this model and the estimate of the libration angle we can obtain a time constant (or a damping constant) for the libration from our relaxation data. Previous work describing the out-of-plane libration of the amide reported typical values for the correlation time of approximately  $\tau_c = 8$  ps. With the assumption that the angle of libration is approximately  $10^\circ$ , we also obtain a correlation time of the same order of magnitude (approximately 14 ps, 60 GHz or  $2\text{ cm}^{-1}$ ) for a  $T_1$  of 1 s. For relaxation times of 10 ms to 500 s the correlation times range from 1.4 ns to 140 fs (600 MHz to 6 THz, or 0.2 to  $200\text{ cm}^{-1}$ ). For comparison, computational studies of proteins using molecular dynamics or normal mode methods have found a number of modes with frequencies in the  $1\text{--}100\text{ cm}^{-1}$  range.<sup>10,11,51,52</sup> Many of the modes that involve rotations or distortions of the amide have frequencies around or below  $50\text{ cm}^{-1}$ .

Since our temperature-dependent data clearly indicate that the motion is not an activated process but a librational process, it is worthwhile to discuss how  $T_1$  is related to temperature. From the equations above and rewriting eq 8 as  $\langle\theta_\eta^2(T)\rangle =$

$\langle\theta_\eta^2(0)\rangle T$  (eq 10), the temperature dependence of  $T_1$  is given by

$$\frac{1}{T_1(\Omega')} \cong \frac{15(eEqQ)^2 \langle\theta_\eta^2(0)\rangle^2 T^2}{16\hbar^2 D} \quad (11)$$

From eq 11, the inverse of  $T_1$  vs the square of temperature should produce a straight line with a slope equal to quotient of the angular excursion and the diffusion constant. In Figure 6, we show that such a plot for the amide-deuterated sample is relatively linear, but the  $\alpha$ -labeled compound shows some deviation. The change in libration angle with temperature for the amide-deuterated sample was found from the width in residual density in the line shape collected at two temperatures and is comparable to that found in the study of Usha *et al.*<sup>38</sup> Using the value for  $\langle\theta^2(0)\rangle$  from our data,  $1.5 \times 10^{-4}\text{ rad}^2/\text{K}$  ( $1.1 \times 10^{-4}\text{ rad}^2/\text{K}^{38}$ ), and the quadrupole coupling constant of 200 kHz, the slope obtained from the fit gives  $1.4 \times 10^{-5}$  for the amide-deuterated sample giving a diffusion constant of  $2.9 \times 10^8\text{ s}^{-1}$ . The slope for the  $\alpha$ -deuterated sample is  $5.4 \times 10^{-5}$ , although it appears to deviate from linearity. This faster relaxation rate and slope for the  $\alpha$ -deuterated compound is consistent with a smaller moment of inertia, which predicts a greater amplitude in the angular excursion or a stronger frictional force or both. Careful line-shape analysis of nylon 66 from previous work of English *et al.* indicates that a larger angular excursion for the methylenes is most likely to be responsible for this difference between the amide and the flanking methylenes.<sup>29</sup>

#### Dihedral Angles and Spin–Lattice Relaxation Rates. In

summary, our data suggest that some but not all amides in crystalline environments show a slow librational process on the time scale which leads to spin–lattice relaxation for the amidic deuteron. All amides that exhibit relaxation have flanking alkyl groups (larger than a methyl group), and most have the flanking dihedral values near  $-60^\circ$ , so that gauche interactions are expected.

Assuming that the angular excursion is similar for amides with different spin–lattice relaxation rates, which is supported by crystallographic thermal factors, the difference in these spin–lattice relaxation rates is due to the difference in friction coefficient or diffusion constants. These constants can be defined in molecular terms using the fluctuation–dissipation theorem, which states that the diffusion constant is related to the correlation function of the random fluctuating field. Diffusion constants for solute molecules have been calculated; the random fluctuating field is usually considered in terms of random collisions of a solute molecule with the solvent molecules, and the diffusion constant is related to the autocorrelation function of the particle’s velocity.<sup>53–55</sup> In a crystalline solid, these collisions would not be spatially random. The fluctuating field experienced by the amidic deuteron is related to its neighbor’s motion, the adjacent methylene groups, and crystallographic neighbors. If the random fluctuating field is harmonic and at a frequency very different than the frequency of the amide libration, its spectral density will not be effective in damping. If the random fluctuating field is stochastic or strongly overdamped, it could have significant overlap with the librational frequency resulting in a strong frictional force or small diffusion constant. The difference between the fast relaxing and the slow relaxing amides is proposed to be the extent of coupling to modes in flanking regions. It is striking that flanking dihedral groups are needed for the motion to appear on the NMR time scale. We observed a correlation between flanking dihedral angles and relaxation rates of the amidic

deuteron for a wide range of amides. For the fast relaxing deuterons, with  $\phi$  and  $\psi$  values around  $-60^\circ$ , the  $\alpha$ -methylene protons eclipse amidic oxygen and are gauche to the amidic proton (Figure 7). The groups adjacent to the  $\alpha$ -methylene groups are also gauche to their neighbors. We conclude that the flanking dihedral angles in secondary amides somehow influence the damping of the out-of-plane libration of the amide plane, possibly involving nonbonded interactions such as the eclipsing and gauche.

In a normal mode dynamics simulation of bovine pancreatic trypsin inhibitor, the displacements of  $\phi$  and  $\psi$  were correlated against each other and against the dihedrals of adjacent amides.<sup>51</sup> Significant correlations for  $\alpha$ -helix secondary structure were observed for dihedrals four units away in either direction, but notably absent for the  $\beta$ -sheet secondary structure. The correlation value of the  $\phi/\psi$  angle of the central amide unit,  $\langle \Delta\phi_0 \Delta\psi_0 \rangle$ , was  $-0.30$  for an  $\alpha$ -helix and  $0.0$  for a  $\beta$ -sheet.

On the basis of our observations one might expect damping and modification of amide librational dynamics to encapsulate the slower time scales (nanosecond) for  $\alpha$ -helical structures; this damping might be important for facilitating an even slower, larger amplitude and more functionally relevant motions. In contrast,  $\beta$ -structures are predicted to exhibit stiffer and more harmonic motions which remain on a time scale far separated from that of functionally relevant processes. This predicted difference in the time scales of backbone motions should be tested with SSNMR studies on selectively labeled proteins.

## Conclusions

We have measured librational dynamics of amide groups in crystalline solids and compared these motions with a variety of structural and electronic properties. We observed fast deuterium spin–lattice relaxation rates associated with a damped or slow amide libration when the amide is alkyl substituted on both sides and furthermore if both dihedral angles adjacent to the amide,  $\phi$  and  $\psi$ , were approximately  $-60^\circ$ . We also found that  $^{13}\text{C}$  CSA, deuterium quadrupolar coupling constants, and CO and NH stretch frequencies are not particularly sensitive to the hydrogen bond geometry or modest changes in length. We postulate that the difference in deuterium spin–lattice relaxation rates for the various amides is related to the anharmonicity of the amide deflection and consequent damping of the motion, resulting in significant spectral density on the NMR time scale. The damping is apparently unrelated to hydrogen bonding but strongly related to flanking alkyl groups.

**Acknowledgment.** We gratefully acknowledge Sharon Rozovsky for quadrupolar order measurements and for carefully reading the manuscript. We also thank Dr. Titan Gu for advice on CSA simulations. We thank Professor Richard Wittebort at the University of Louisville, Kentucky, for conversations about the dynamics of the amide unit; Professor Ged Parkin, Columbia University, for collecting X-ray data and solving the *N-tert-butylpropionamide* crystal structure; Dr. Ivan Vulic' at DSM, The Netherlands, for providing a sample of the polyamide-4,6 model compound; and Dr. Nancy Triggs, Notre Dame, and Professor James Valentini, Columbia University, for discussion of amide hydrogen bonding.

**Supporting Information Available:** Spin–lattice relaxation rates and CSA tensor elements (4 pages). Ordering information is given on any current masthead page.

## Abbreviations

SSNMR                      solid state NMR

$T_1$	spin–lattice relaxation time
CPMAS	cross polarization–magic angle spinning
CSA	chemical shift anisotropy
H-bond	hydrogen bond
HPMDB	heptamethylenedibenzamide
HXMDB	hexamethylenedibenzamide
HXMDA	hexamethylenediacetamide
HXMDP	hexamethylenedipropionamide
polyamide-4,6	1,6-diazacyclododecane-7,12-dione
cyclic monomer	1,8-diazacyclotetradecane-2,7-dione
caprylolactam	2-azacyclononanone
caprolactam	2-azacycloheptanone
lauryllactam	2-azacyclotridecanone
homozaadamantone	4-azatricyclo[4.3.1.1]undecan-5-one
nylon-4,4	tetramethylenedibutylamide
nylon-6,6	hexamethylenedihexamide

## References and Notes

- Englander, S. W.; Englander, J. J.; McKinnie, R. E.; Ackers, G. K.; Turner, G. J.; Westrick, J. A.; Gill, S. J. *Science* **1992**, *256*, 1684–1687.
- Kossiakoff, A. A. *Nature* **1982**, *296*, 713–721.
- Austin, R. H.; Beeson, K. W.; Eisenstein, L.; Frauenfelder, H.; Gunsalus, I. C. *Biochemistry* **1975**, *14*, 5355–5373.
- Stezowski, J. J.; Peachey, N. M.; Goebel, P.; Eckhardt, C. J. *J. Am. Chem. Soc.* **1993**, *115*, 6499–6505.
- Frauenfelder, H.; Sligar, S. G.; Wolynes, P. G. *Science* **1991**, *254*, 1598–1603.
- Diott, D. D. *Optical Phonon Dynamics in Molecular Crystals*; Annual Reviews: 1986.
- Fanconi, B.; Small, E. W.; Peticolas, W. L. *Biopolymers* **1971**, *10*, 1277–1298.
- Bee, M. *Quasielastic Neutron Scattering*; 1st ed.; Adam Hilger: Bristol, 1988.
- Jonscher, A. K. *J. Mater. Sci.* **1981**, 2037–2060.
- Pleiss, J.; Jahnig, F. *Biophys. J.* **1991**, *59*, 795–804.
- Perahia, D.; Levy, R. M.; Karplus, M. *Biopolymers* **1990**, *29*, 645–677.
- Spieß, H. W. *NMR: Basic Princ. Prog.* **1980**, *15*, 59–213.
- Vold, R. R.; Vold, R. G. *Adv. Magn. Opt. Resn.* **1991**, *16*, 85–171.
- Griffin, R. G. *Methods of Enzymology*; Academic Press: New York, 1981; Vol. 72, pp 108–174.
- Rabbani, S. R.; Edmonds, D. T.; Gosling, P. J. *Magn. Reson.* **1987**, *72*, 422–433.
- Brown, T. L.; Butler, L. G.; Curtin, D. Y.; Hiyama, Y.; Paul, I. C.; Wilson, R. B. *J. Am. Chem. Soc.* **1982**, *104*, 1172–1177.
- Bersohn, R. *J. Chem. Phys.* **1960**, *32*, 85–88.
- Hunt, M. J.; Mackay, A. L. *J. Magn. Reson.* **1976**, *22*, 295–301.
- Marks, B. S.; Schweiker, G. C. *J. Polym. Sci.* **1960**, *43*, 229–239.
- Gaymann, R. J.; Harkema, S. J. *Polym. Sci. Phys. Ed.* **1977**, *15*, 587–590.
- Vulic', I.; Hooft, R. W. W.; Kroon, J. J. *Crystallogr. Spectrosc. Res.* **1993**, *23*, 917–920.
- Herzfeld, J.; Berger, A. *J. Chem. Phys.* **1980**, *73*, 6021–6030.
- The Role of Hydrogen Bonding in Molecular Assemblies*; Bernstein, J., Etter, M. C., Leiserowitz, L., Eds.; VCH: New York, 1994.
- Leiserowitz, L.; Tuval, M. *Acta Crystallogr.* **1978**, *B34*, 1230–1247.
- Berkovitch-Yellin, Z.; Leiserowitz, L. *J. Am. Chem. Soc.* **1980**, *102*, 7677–7690.
- Dauber, P.; Hagler, A. T. *Acc. Chem. Res.* **1980**, *13*, 105–112.
- Taylor, R.; Kennard, O.; Versichel, W. *Acta Crystallogr.* **1984**, *B40*, 280–288.
- Benedetti, E.; Ciajolo, M. R.; Corradini, P. *Eur. Polym. J.* **1973**, *9*, 101–109.
- Hirschinger, J.; Miura, H.; Gardner, K. H.; English, A. D. *Macromolecules* **1990**, *23*, 2153–2169.
- Dunitz, J. D.; Winkler, F. K. *Acta Crystallogr.* **1975**, *B31*, 251–263.
- Ando, S.; Ando, I.; Shuji, A.; Ozaki, T. *J. Am. Chem. Soc.* **1988**, *110*, 3380–3386.
- Asakawa, N.; Kuroki, S.; Kurosu, H.; Ando, I.; Shoji, A.; Ozaki, T. *J. Am. Chem. Soc.* **1992**, *114*, 3261–3265.

- (33) Gu, Z.; Zambrano, R.; McDermott, A. *J. Am. Chem. Soc.* **1994**, *116*, 6368–6372.
- (34) Llinas, M.; Wilson, D. M.; Klein, M. P. *J. Am. Chem. Soc.* **1977**, *99*, 6846–6850.
- (35) Lumsden, M. D.; Wasylishen, R. E.; Eichele, K.; Schindler, M.; Penner, G. H.; Power, W. P.; Curtis, R. D. *J. Am. Chem. Soc.* **1994**, *116*, 1403–1413.
- (36) Winkler, F. K.; Dunitz, J. D. *Acta Crystallogr.* **1975**, *B31*, 268–269.
- (37) Chiba, T. *Bull. Chem. Soc. Jpn.* **1965**, *38*, 259–263.
- (38) Usha, M. G.; Peticolas, W. L.; Wittebort, R. J. *Biochemistry* **1991**, *30*, 3955–3962.
- (39) Henry, E. R.; Szabo, A. *J. Chem. Phys.* **1985**, *82*, 4753–4761.
- (40) Lonsdale, K. *Acta Crystallogr.* **1961**, *14*, 37–42.
- (41) Swaminathan, S.; Craven, B. M.; McMullan, R. K. *Acta Crystallogr.* **1984**, *B40*, 300–306.
- (42) Greenfield, M.; Vold, R. L.; Vold, R. R. *Mol. Phys.* **1989**, *66*, 269–298.
- (43) Mack, J. W.; Torchia, D. A. *J. Phys. Chem.* **1991**, *95*, 4207–4213.
- (44) Kinsey, R. A.; Kintanar, A.; Oldfield, E. *J. Biol. Chem.* **1981**, *256*, 9028–9036.
- (45) Williams, J. C.; McDermott, A. E. *Biochemistry* **1995**, *34*, 8309–8319.
- (46) Wittebort, R. J.; Szabo, A. *J. Chem. Phys.* **1978**, *69*, 1722–1736.
- (47) Chandrasekhar, S. *Rev. Mod. Phys.* **1943**, *15*, 1–89.
- (48) Szabo, A. *J. Chem. Phys.* **1984**, *81*, 150–167.
- (49) Peticolas, W. L.; Kurtz, B. *Biopolymers* **1980**, *19*, 1153–1166.
- (50) Spiess, H. *J. Chem. Phys.* **1980**, *72*, 6755–6762.
- (51) Levitt, M.; Sander, C.; Stern, P. S. *J. Mol. Biol.* **1985**, *181*, 423–447.
- (52) Brooks, B.; Karplus, M. *Proc. Natl. Acad. Sci. U.S.A.* **1983**, *80*, 6571–6575.
- (53) Straub, J. E.; Borkovec, M.; Berne, B. J. *J. Phys. Chem.* **1987**, *91*, 4995–4998.
- (54) Berne, B. J.; Borkovec, M.; Straub, J. E. *J. Phys. Chem.* **1988**, *92*, 3711–3725.
- (55) Zhang, Y.; Bull, T. E. *Phys. Rev. E* **1994**, *49*, 4886–4902.
- (56) Williams, J. C. Thesis, Columbia University, 1995.